PHYSICAL REVIEW B VOLUME 42, NUMBER 1 1 JULY 1990

Electron-energy-loss and optical-transmittance investigation of $Bi_2Sr_2CaCu_2O_8$

Yun-Yu Wang, Goufu Feng, and A. L. Ritter
Department of Physics, Virginia Tech, Blacksburg, Virginia 24061
(Received 24 January 1990)

The energy-loss function $\mathrm{Im}(-1/\epsilon)$ of $Bi_2Sr_2CaCu_2O_8$ has been measured over the range $E_{\mathrm{loss}}=0.8$ to 80 eV by transmission electron-energy-loss spectroscopy (EELS) (nonimaging). The energy and momentum resolution were 0.1 eV and 0.04 Å^{-1}, respectively. The low-energy spectra ($E_{\mathrm{loss}} \leq 3$ eV) were studied as a function of momentum transfer ($0.1\ \text{Å}^{-1} \leq q \leq 0.3\ \text{Å}^{-1}$). A well-defined peak in the loss function at $E_{\mathrm{loss}} \sim 1$ eV is observed to disperse with momentum proportional to q^2. This excitation is analyzed in terms of both an intracell, charge-transfer exciton model and the free-carrier (plasmon) model. The derived effective mass of the exciton $m_{\mathrm{tot}}/m \simeq 1.0$ is far too small for a localized exciton. Using the free-carrier model and random-phase-approximation expressions for the dispersion coefficient, the carrier density and carrier effective mass can be determined separately. From our data and similar measurements by Nücker *et al.* [Phys. Rev. B **39**, 12 379 (1989)], it is found that the effective mass roughly scales with carrier density. A heuristic model is introduced based on the assumption that low-energy gaps exist in portions of the Fermi surface due to structural instabilities. The model suggests how the effective mass could appear to scale with carrier density and why a single Drude term (with frequency-independent effective mass) does not describe the mid- to far-infrared optical spectra. Finally, the optical transmittance of the EELS sample was measured and the spectra analyzed in terms of the free-carrier model.

The normal-state electronic structure of high-temperature superconductors is a challenging theoretical problem because of the structural complexity of these multicomponent, multiphase systems. Theoretical models for defect-free crystals are difficult to analyze because electron-electron correlations may be significant resulting in the breakdown of the independent particle approximation. Add to these difficulties, the perturbation of the electronic structure produced by defects and inhomogeneities in the crystal structure, and one is faced with the daunting problem of separating intrinsic from defect-mediated extrinsic factors in the experimental data. Because of this complexity, most optical studies of the electronic structure have concentrated on fitting the spectra to phenomenological models, such as the Drude and Lorentz oscillator expressions. Considerable controversy exists regarding even the proper phenomenology.[1] One question centers on the nature of a reflectivity edge typically seen in the mid- and near-infrared energy range in many high-temperature superconductors. This edge translates to a plasmonlike excitation at ~ 1 eV in electron energy-loss spectra. The controversy revolves on whether this excitation should be described by a free-carrier, Drude model (with, possibly, frequency dependent effective mass),[2] or whether it is better modeled by a Lorentz oscillator with center frequency in the far- to mid-infrared.[3,4] In order to explore this question further, we have studied $Bi_2Sr_2CaCu_2O_8$ by high energy, transmission election-energy-loss-spectroscopy (EELS) and by transmittance measurements. We compare our EELS measurement with a similar study by Nücker *et al.*[5] ("KG" for Karlsruhe group) and find significant differences in the spectra below $E_{\mathrm{loss}} \sim 2$ eV which we suggest arises from small variations in the stoichiometry of the samples. We analyze our EELS and optical data in terms of both the Drude and Lorentz oscillator models. The Drude model gives a better description of our data but would not be consistent with far-infrared optical measurements.[4] We suggest a heuristic model of the underlying electronic structure in these materials which may explain why a single phenomenological model does not describe the optical spectra over the entire frequency range.

The first part of this paper discusses the preparation and characterization of the samples and describes the EELS and optical spectrometers. The EELS data is presented next and fit by a sum of Drude plus Lorentz oscillator expressions to model the dielectric constant. Following this, we discuss the implications of assuming that the 1-eV excitation in EELS arises from the free-carrier response to the probe versus assuming this excitation is associated with excitons. Next, a heuristic picture of the electronic structure is presented which harmonizes the free-carrier versus local-oscillator descriptions of the data. Finally, the optical transmittance spectra is discussed in terms of the dielectric function derived from the EELS data. Our transmittance data is not consistent with the analysis by Reedyk *et al.*[4] of their far-infrared measurements on $Bi_2Sr_2CaCu_2O_8$. We argue that, again, small variations in the stoichiometry of the samples can explain the differences in the optical spectra.

Our samples were prepared by a flux method from Bi_2O_3, $SrCO_3$, CaO, and CuO in the proper molar proportion 2:2:1:2 using a procedure very similar to the method reported by Schneemeyer *et al.*[6] A highly orient-

ed cluster of crystallites formed on the KCl crystal. The KCl was dissolved in water and a thin crystallite was separated from the cluster and mounted on an electron microscope grid. An inductance measurement on a thicker crystallite showed that the superconducting transition temperature was ~ 78 K with a width of 2 K. The transition temperature of the EELS sample could not be determined accurately due to a temperature-dependent background from the sample holder. An x-ray-diffraction analysis of the sample showed $\sim 90\%$ of the sample was in the 2:2:1:2 phase ($c = 30$ Å) while the remaining fraction was in the $Bi_2Sr_2CuO_6$ phase ($c = 24$ Å). The c axis of the sample is perpendicular to the film and all measurements reported in this paper have **q** perpendicular to the c axis, thus, giving the component of the dielectric tensor in the Cu-O_2 planes.

The electron-energy-loss measurements were taken with a high-resolution, transmission electron-energy-loss spectrometer (nonimaging) similar to the instrument described by Gibbons *et al.*[7] The incident-beam energy is 80 KeV and the energy resolution is 0.10 eV (FWHM). The momentum resolution is 0.04 $Å^{-1}$ (FWHM). The optical transmittance measurements were taken on a modified Perkin-Elmer, prism-grating spectrometer, using chopped radiation and lock-in detection. The energy range was 0.2–6.2 eV.

The energy-loss spectra $\mathrm{Im}(-1/\epsilon)$, for $q = 0.1$ $Å^{-1}$ from $E = 0$ to $E = 80$ eV is shown in Fig. 1. The quasielastic peak centered at $E = 0$ is removed from the data and the data has been extended to zero energy by fitting the spectra from 0.8 to 3.0 eV with a Drude term plus a Lorentz oscillator. This fitting procedure will be analyzed later in this paper. The raw data is corrected for multiple scattering and placed on an absolute scale by taking $\mathrm{Re}(1-1/\epsilon)=1$ (for a conductor) and satisfying the f-sum rule. The data has been extended from $E = 80$ eV to infinity assuming $\mathrm{Im}(-1/\epsilon) \sim 1/E^3$. For the sum rule, we assumed there were 284 electrons per unit cell with atomic binding energies less than 80 eV. The significant features in the loss spectra for 3 eV $< E <$ 80 eV are in good agreement with the energy-loss measurements of KG. There is a sharp rise in the loss function at 3.4 eV; a shoulder on this abrupt increase at 7 eV, the bulk valence plasmon peak at ~ 20 eV, and the spin-orbit split Bismuth 5d doublet at 28 eV and 30 eV. A prominent shoulder at 33 eV which is seen by KG does not appear in our data. We did see this shoulder in the spectra of thicker samples and suspect it may be due to incomplete removal of double scattering. Our spectra in the range 0.7–3.0 eV is significantly different from the results of KG. They find the maximum value of the loss function for the 1-eV excitation is $\mathrm{Im}(-1/\epsilon)=0.3$ at $q = 0.1$ $Å^{-1}$, while we find for the same momentum $\mathrm{Im}(-1/\epsilon)=0.17$. We find the same width for the 1-eV excitation, but the dispersion of this peak with momentum is much weaker in our sample. The emphasis of this paper will be on this region of energy, $E \leq 3.0$ eV, since the Cu-O_2 sheets are thought to dominate the spectra in this range. We believe that our spectra differ from the spectra measured by KG in this energy range because the concentration of holes in the Cu-O_2 planes is different in the two samples. The hole concentration is sensitive to the stoichiometry of the material which can vary over a limited range (without changing the basis crystal structure) due to differences in the sample preparation procedure. The implications of this difference in the energy-loss spectra will be analyzed further.

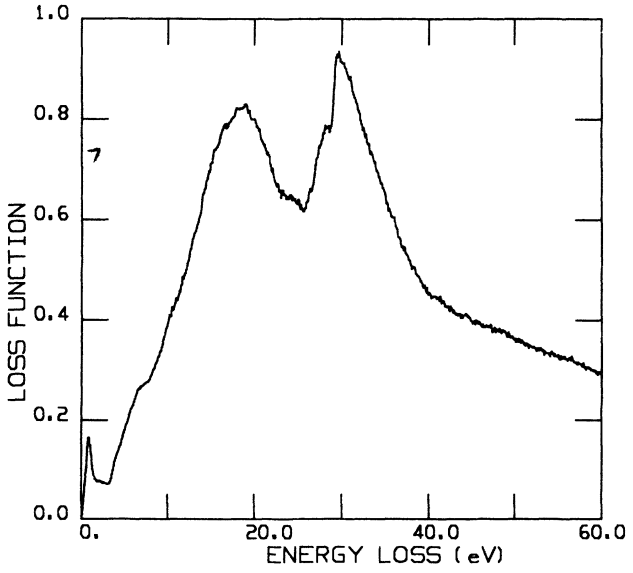

FIG. 1. The loss function, $\mathrm{Im}(-1/\epsilon)$, as a function of energy for momentum $q = 0.1$ $Å^{-1}$.

The energy-loss spectra from 0.8 to 3.0 eV for five different momentums are shown in Fig. 2. The quasielastic peak and instrumental background obscure the spectra below 0.8 eV. In order to scale the data properly, it is necessary to know the functional dependence of the loss function as E goes to zero. In order to perform this extrapolation, the energy-loss data was fitted by a Drude term plus a Lorentz oscillator:

$$\epsilon = \epsilon_\infty - \frac{\omega_p^2}{\omega^2 + i\Gamma\omega} - \frac{f_1^2}{\omega^2 - \omega_1^2 + i\Gamma_1\omega} . \quad (1)$$

The Drude term represents the 1 eV excitation while the oscillator models the slowly varying background. The solid lines in Fig. 2 are the generated fits to the data based on Eq. 1. An important question, and a subject of some controversy, is whether the 1-eV excitation is due to free carriers or is itself better modeled by a local oscillator. This question will be addressed later in the paper. The fitting parameters for $q = 0.1$ $Å^{-1}$ are $\epsilon_\infty = 5.15$, $\hbar\omega_p = 2.5$ eV, $\hbar\Gamma = 0.75$ eV, $\hbar f_1 = 3.5$ eV, $\hbar\omega_1 = 2.7$ eV, and $\hbar\Gamma_1 = 2.9$ eV. As the momentum transfer increases, the "plasmon" peak disperses upward in energy and broadens. The dispersion of the peak as a function of q^2 is shown in Fig. 3. The results of KG are shown as the dashed line. Fitting the data by the expression

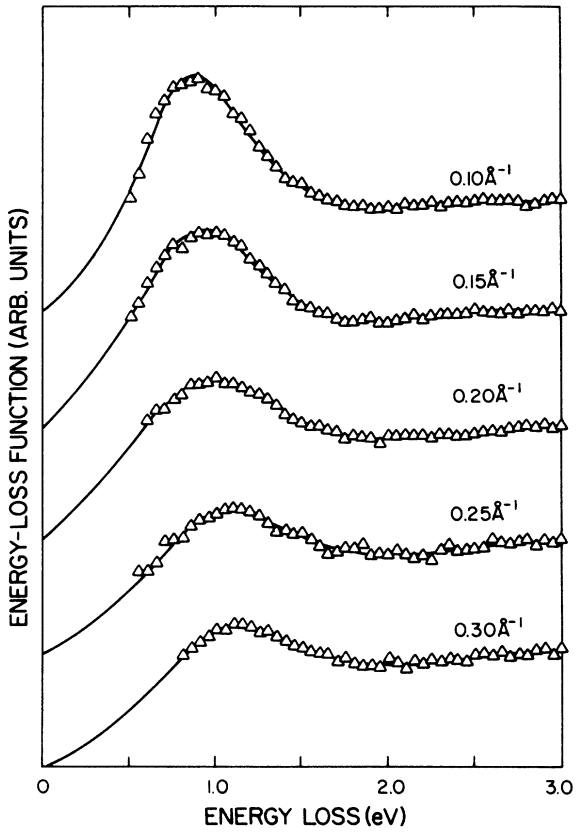

FIG. 2. The energy-loss spectrum for five different momentum q from 0.10 Å^{-1} to 0.30 Å^{-1} with the energy range from 0 to 3.0 eV. The solid lines are from fitting the data by a Drude model and a Lorentz oscillator.

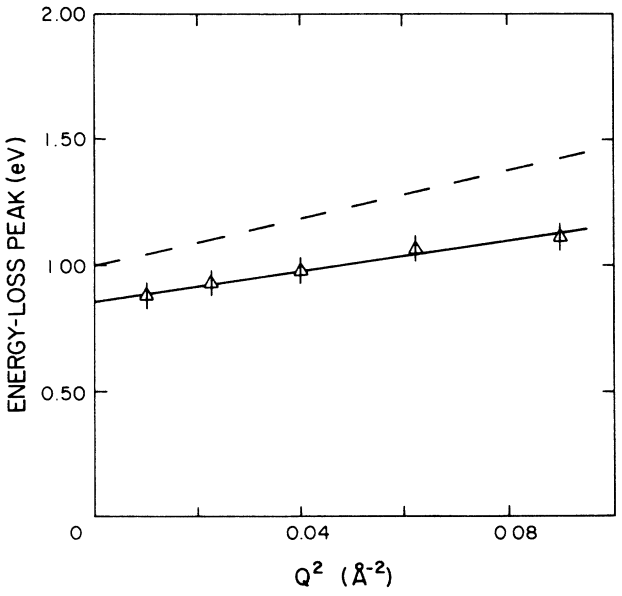

FIG. 3. The dispersion of the energy-loss peak as a function of momentum squared. The dashed line is the data from Nücker *et al.* (Ref. 5).

$$E_p'(q)=E_p'(0)+\frac{\hbar^2\alpha}{m}q^2 , \tag{2}$$

we find $E_p'(0)=0.9$ eV and $\alpha=0.4\pm0.1$, while KG found $E_p'(0)=1.0$ eV and $\alpha=0.6$. Thus, we find approximately the same screened plasmon energy and plasmon width as KG, but the magnitude of the peak in our data is less than the magnitude seen by KG. Also, our dispersion coefficient is 30% smaller than the coefficient measured by KG.

One possible explanation of the 1-eV energy-loss excitation is to associate it with some type of charge-transfer exciton with binding energy of ~0.1 eV. In this case, the fitting parameter α from Eq. 2 is $0.5m/(m_1+m_2)$ where for conventional Mott-Wannier and Frenkel excitons, m_1 and m_2 are electron and hole effective masses. From our data $(m_1+m_2)/m=1.3$ while the KG data give $(m_1+m_2)/m=0.8$. In silicon and germanium this ratio is ~1.0 while in wide-band gap insulators, such as LiF, it is ~4. One possible explanation for this excitation is that it represents an intracell, charge transfer reaction between neighbor cations and anions[8] which presumably would be quite localized and, therefore, have a substantial effective mass. The energy-loss results for the mass of the exciton are too low for such a model. Also, for an intracell excitation it is difficult to understand why the mass ratio differs so drastically between two sets of data taken on samples which may differ in stoichiometry by less than 20%. We now consider the dispersion of this excitation from the point of view that it arises from free carriers.

The free-carrier, screened plasmon energy at $q=0$ can be written in atomic units (Ry=27.2 eV)

$$(\hbar\omega_0')^2=\frac{4\pi n}{\epsilon_\infty m^*/m} , \tag{3}$$

while in the RPA the dispersion coefficient is

$$\alpha=\frac{3}{10}\frac{mv_F^2}{\hbar\omega_0'} . \tag{4}$$

We use the three-dimensional, rather than two-dimensional, expressions for the plasmon because **q** is nearly perpendicular to the c axis. Assuming a cylindrical Fermi surface for holes in the $Cu\text{-}O_2$ planes, the product of the dispersion coefficient and the plasma energy can be written

$$\alpha\hbar\omega_0'=\frac{3\pi nc}{10(m^*/m)^2} , \tag{5}$$

where c is the dimension of the unit cell along the c axis. The parameters n and m^* are obtained now from Eqs. (3) and (5), but first the accuracy and limitations of these two equations should be considered. The expression for the screened plasmon energy, Eq. (3), is in good agreement with measurements on many different materials,[9] but serious discrepancies exist between the observed dispersion coefficient and the RPA prediction even in simple, free-electron metals.[10] In some cases the slope of the dispersion with q^2 is not constant. In both our data and KG's measurements, the excitation frequency is proportional to

q^2 over the full momentum range. If the excitation is a free-carrier plasmon, then one expects the dispersion constant will be proportional to $(E_F)/(\hbar\omega_0' m^*/m)$. The proportionality constant may be different from $\frac{3}{5}$ predicted by RPA, but n and m^*/m simply scale with this proportionality constant when Eqs. (3) and (5) are solved. Thus, the qualitative correlation between n and m^*/m which we derive below from combining our results with the measurements of KG is insensitive to the exact value of this constant. So, based on the RPA constant, the KG data gives $m^*/m=1.2$ and $n=4.2\times10^{21}/\text{cm}^3$ (0.5 holes /Cu-O_2 layer) while our measurements give $m^*/m=2.2$ and $n=9.7\times10^{21}/\text{cm}^3$ (1.0 hole/Cu-O_2 layer). Again, the quantitative values of these parameters, though they are reasonable, should not be taken too seriously since they depend on the dubious RPA constant. But the approximate scaling of m^* with n is a more robust implication of this model and will be considered in more detail now.

The rough proportionality between m^* and n predicted by the Free-carrier model for the 1-eV excitation has arisen in the interpretation of other optical measurements. Studies of $(La_{1-x}Sr_x)_2CuO_4$ (Ref. 11-13) find that the reflectivity edge, which marks the screened plasmon energy, is nearly independent of x while the carrier concentration measured by the Hall effect is proportional to x—again, implying that the ratio m^*/n remains constant while n varies. A recent exhaustive investigation of $Bi_2Sr_2Ca_{n-1}Cu_nO_y$ by Madea *et al.*[14] using reflectivity and Hall effect measurements found that in 2:2:1:2 the screened plasmon energy did not change appreciably when they varied n. The common feature in these two experiments was a pinned reflectivity edge as the carrier concentration varied suggesting at least two interpretations: that m^*/n was constant or that the reflectivity edge was due to a localized oscillator. Assuming, for the sake of argument, that the 1-eV excitation seen in EELS and the reflectivity edge observed at the same energy are associated with free-carriers, then different experiments point to the conclusion that m^*/n remains roughly constant when n is varied. If true, this implies that m^* goes to zero in the limit of a half-filled band when n is zero. In most systems, there is a metal-insulator transition before reaching this limit and the model of free-carriers breaks down. But in $(La_{2-x}Sr_x)_2CuO_4$ we find from the reflectivity and Hall effect data of Suzuki[11] that m^* is proportional to n over the reasonably wide range $0.04\le x\le0.20$. We propose now a heuristic model for the electronic structure of carriers in the Cu-O_2 sheets which suggests how m^* might appear to scale with n and which may shed light on the controversy regarding the proper model for the 1-eV excitation.

We first assume that for large enough doping the carriers in the Cu-O_2 sheets can be described by an independent particle, band model. To be concrete, we will assume a tight-binding, near-neighbor band

$$\epsilon_k=-2t[\cos(k_x)+\cos(k_y)]-\mu \tag{6}$$

though our argument isn't sensitive to the exact shape of the band except that it be strongly nested when μ, the chemical potential, is zero (half-filled band). Hirsch[15] has calculated the Fermi surface for various band fillings from Eq. 6 (see Fig. 4). There is significant nesting of the Fermi surface between the quarter-filled band (electron filling $\rho=0.5$) and the half-filled band (electron filling $\rho=1.0$). Our second assumption is that the crystal structure is unstable to distortion, whether it is due to spin density wave (SDW), charge density wave (CDW), or electron-electron correlation is immaterial, which opens gaps in the nested segments of the Fermi circumference. When n, the hole density, is large ($\rho<0.5$); these distortions are weak since only limited segments of the Fermi circumference are nested. But, as n tends to zero (the half-filled band) and nesting becomes more significant, then the distortion increases and longer segments of the Fermi circumference lie in the gap. Our last assumption is that the magnitude of these distortion gaps is in the mid- to far-infrared energy range ($E_{\text{gap}}\le0.5$ eV) and is much less than the bandwidth. It then follows from this last assumption[16] that the local effective mass of states on the edge of the gap is proportional to the gap, $m^*/m\sim E_{\text{gap}}/\text{bandwidth}$. Therefore, the mass of states on the Fermi circumference can vary widely from $m^*/m\le0.1$ to $m^*/m\ge1$. We do not know of any calculation of the complex dielectric constant from such a model and, so, will conjecture what connection might exist between this model and different phenomenological fits of optical data to sums of Drude plus Lorentz oscillators. Our model, then, is a two-dimensional Fermi circumference with small gaps in the segments lying across the four, symmetry-related [110] directions. The effective masses of electrons in states near the distortion gaps are quite small. The relative lengths of segments without gap to segments with gaps will decrease as carrier concentration goes to zero and the Fermi circumference becomes

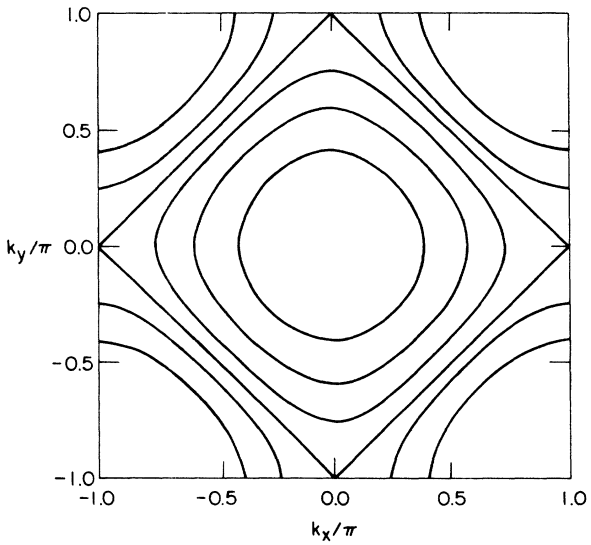

FIG. 4. Fermi surfaces for electrons on a two-dimensional square lattice with nearest-neighbor hopping only (Ref. 15). Band fillings are $\rho=0.25$, 0.5, ... 1.5 starting from the inner surface. The Fermi surface for the half-filled case is nested.

strongly nested. Considering now low energy, intraband excitations ($E_{\rm loss} \leq 2$ eV), we suggest that one phenomenological description of the optical response is to ignore the distortion gaps and use the Drude model for the holes in this band. This approach should work best when $E_{\rm loss}$ is considerably larger than the distortion gaps. The effective mass in the expression for the plasma frequency then would be some average over the Fermi circumference. When the hole concentration is large and most of the circumference is gapless, then the effective mass will be its maximum value ($m^*/m \gtrsim 1$). As the hole concentration decreases, the average effective mass will be weighted more strongly by segments where the distortion gaps exist and the average effective mass will decrease. Thus, it is conceivable that the ratio m^*/n as a function of n remains roughly constant. This must be checked by explicit calculations from the model. When the optical measurements are in the mid- and far-infrared optical range such that the excitation energy is comparable to or less than the distortion gaps, then a phenomenological model based on a single Drude term must surely break down. It is not surprising that a Drude term representing electrons on the gapless segment of the Fermi circumference plus Lorentz oscillators to model transitions across the gaps gives a better description of the optical spectra. In this case, one expects to see a transfer of oscillator strength from the Drude term to the local oscillators as the carrier concentration goes to zero. In summary, our heuristic model suggests why the EELS spectra for energies $E_{\rm Loss} \geq 0.8$ eV can be fit so well by a Drude model and why the effective mass apparently scales with hole concentration. It also is consistent with the observation that mid- and far-infrared data can not be fit by a single Drude oscillator with frequency independent relaxation. The Drude model predicts that the reflectivity will smoothly increase to unity below the plasma frequency, but the measured refectivity has several bumps and shoulders on top of a Drudelike behavior. In our model these perturbations of the monotonically increasing reflectivity are associated with the distortion gaps. Some of these features are not very reproducible[17] which is consistent with our expectation that the gaps on the Fermi circumference will be quite sensitive to local inhomogeneities in the stoichiometry of the sample. Next, we analyze the optical transmittance of the same sample on which energy loss measurements were made and find that it is consistent with our model.

The optical transmittance of our sample in the range 0.2–6.2 eV is the solid line shown in Fig. 5(a). Taking the parameters derived from fitting the data by Eq. 1 (modeling the 1-eV excitation by a Drude term), we have calculated the transmittance from the expression

$$T(\omega)=\frac{A}{A_T}\frac{|1-\tilde{r}^2|^2}{|1-\tilde{r}^2\exp[-2i\beta]|^2}\exp\left[\frac{-2\omega kd}{c}\right]+T_0\ , \tag{7}$$

where d=thickness, $\beta=\omega\tilde{n}d/c$, $\tilde{r}=(\tilde{n}-1)/(\tilde{n}+1)$, $\tilde{n}=n-ik$, and n and k are the optical constants (related to ϵ_1 and ϵ_2 by standard expressions). The area ratio A/A_T takes into account that only a fraction of the sample illuminated by the infrared beam is thin enough to transmit a significant intensity of radiation. The thickness of this transmitting area was set equal to the thickness $d=500$ Å, derived from analysis of the EELS data. The constant T_0 is to correct for pinholes in the samples. The dashed line in Fig. 5(a) is our calculated transmittance based on the parameters from Eq. 1 assuming $A/A_T=0.25$ and $T_0=0.07$. The fit is reasonably good considering that only A/A_T and T_0 are free parameters. In Fig. 5(b) we compare the reflectivity measured by Takagi *et al.*[18] (solid line) with our calculation of the reflectivity (dashed line), again based on parameters derived from Eq. 1. In this case there are no free parameters and the two measurements are in qualitative agreement. Reedyk *et al.*[4] measured the reflectivity of 2:2:1:2 in the far infrared optical range and fit their data to a low-energy Drude term with a very small relaxation rate ($\Gamma \simeq 0.009$ eV) plus two mid-infrared oscillators. The dashed-dotted line in Fig. 5(a) is the transmittance below

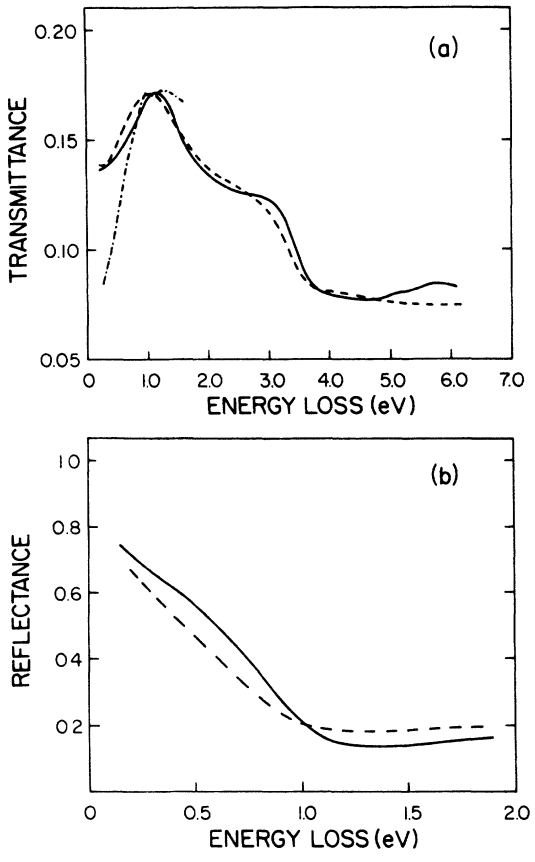

FIG. 5. (a) The solid line is the optical transmittance spectrum of the same sample on which the energy loss measurements were taken. The dashed line is the transmittance calculated from a model based on the energy-loss data. The dot-dashed line is the transmittance calculated from a model based on the far infrared measurements of Reedyk *et al.* (Ref. 4). (b) The dashed line is the reflectance spectrum calculated from a model based on the energy-loss data. The solid line is the reflectance data of Takagi *et al.* (Ref. 18).

1 eV based on their parameters. In this case, we assumed $D=500$ Å, $A/A_T=0.10$, and $T_0=0.07$, but adjusting these parameters did not improve the fit. The narrow plasmon and relatively narrow, mid-infrared oscillators always gave a sharper drop in the low-energy transmittance than we observe. Within the context of the heuristic model just presented, the measurements of Reedyk *et al.* can be brought into consonance with our results if one assumes the carrier density in their samples is less than the density in ours. Then, gaps would exist over a larger fraction of the Fermi circumference in their case and would contribute the sharp, narrow structure they observe which is absent in our transmittance spectra. The preceding analysis of the carrier density in our sample suggests that it is quite high so that our explanation for the lack of sharp structure is self consistent.

In conclusion, the energy-loss function and optical transmittance of $Bi_2Sr_2CaCu_2O_8$ has been measured and the low-energy ($E \leq 3$ eV) spectra has been analyzed in detail. A well-defined peak in the loss function at ~ 1 eV is observed to disperse as the square of the momentum transferred. If this excitation is some form of exciton, then the total mass of the exciton is $m^*/m \lesssim 1.3$ which is too small for a well localized, intracell charge transfer exciton. We also analyzed our measurements and the data of Nücker *et al.* assuming the excitation was a free-carrier plasmon. In this case, the effective mass of the carriers appears to scale with the carrier density. We introduced a heuristic model of the electronic structure of carriers in the $Cu\text{-}O_2$ planes which provides a basis for understanding this scaling behavior. In addition, the model gives some insight into the discordance between our optical measurement and the study by far infrared reflectivity of the same material by Reedyk *et al.* Obviously, a rigorous formulation of this model is necessary before it can be tested more stringently.

We gratefully acknowledge stimulating discussions with T. K. Lee, Liam Coffey, Yaojing Qian, and David Tanner. We also would like to thank Jerome Long, Z. J. Huang, Michael Annen, and Mark Davis for their assistance in helping us to characterize our samples. Finally, we would like to thank Xerox Webster Research Center for donating the electron-energy-loss spectrometer to Virginia Tech.

[1]For a review of work up to October 1988 see Thomas Timusk and David B. Tanner, in *Physical Properties of High Temperature Superconductors I,* edited by Donald M. Ginsberg (World Scientific, Singapore, 1989), p. 339.

[2]See Z. Schesinger *et al.*, Phys. Rev. Lett. **59**, 1958 (1987); I. Bozovic *et al.*, *ibid.* **59**, 2219 (1987); G. A. Thomas *et al.*, Jpn. J. Appl. Phys. Suppl. **26**, 2044 (1987); J. Orenstein and D. H. Rapkine, Phys. Rev. Lett. **60**, 968 (1988); G. A. Thomas *et al.*, *ibid.* **61**, 1313 (1988); R. T. Collins *et al.*, Phys. Rev. B **39**, 6571 (1989).

[3]See T. Timusk *et al.*, Phys. Rev. B **38**, 6683 (1988); S. L. Herr *et al.*, *ibid.* **36**, 733 (1987); K. Kamarás *et al.*, Phys. Rev. Lett. **59**, 919 (1987); D. A. Bonn *et al.*, Phys. Rev. B **37**, 1547 (1988).

[4]M. Reedyk *et al.*, Phys. Rev. B **38**, 11 981 (1988).

[5]N. Nücker *et al.*, Phys. Rev. B. **39**, 12 379 (1989).

[6]L. F. Schneemeyer *et al.*, Nature **332**, 422 (1988).

[7]P. C. Gibbons, J. J. Ritsko, and S. E. Schnatterly, Rev. Sci. Instrum. **46**, 1546 (1975).

[8]C. M. Varma, S. Schmitt-Rink, and Elihu Abrahams, Solid State Commun. **62**, 681 (1989).

[9]Gerald D. Mahan, *Many-Particle Physics* (Plenum, New York, 1983), p. 433.

[10]M. Raether, in *Excitation of Plasmons and Interband Transitions by Electrons,* Vol. 88 of *Springer Tracts in Modern Physics,* edited by G. Höhler (Springer-Verlag, Berlin, 1980).

[11]Minoru Suzuki, Phys. Rev. B **39**, 2312 (1989).

[12]S. Etemad *et al.*, Phys. Rev. B **37**, 3396 (1988).

[13]M. W. Shafer, T. Penny, and B. L. Olson, Phys. Rev. B **36**, 4047 (1987).

[14]A. Maeda, M. Hase, I. Tsukada, K. Noda, S. Takebayashi, and K. Uchinokura, Phys. Rev. B **41**, 6418 (1990).

[15]J. E. Hirsch, Phys. Rev. B **31**, 4403 (1985).

[16]Charles Kittel, *Introduction to Solid State Physics,* 6th ed. (Wiley, New York, 1986), p. 173.

[17]G. A. Thomas *et al.*, J. Opt. Soc. Am. B **6**, 415 (1989).

[18]H. Takagi *et al.*, Nature **332**, 236 (1988).